

Docking-based 3D-QSAR study for 11 β -HSD1 inhibitors

Jin Hee Lee, Nam Sook Kang* and Sung-Eun Yoo

Center for Drug Discovery Technologies, Korea Research Institute of Chemical Technology, Yu seong-gu, Daejeon 305-600, Republic of Korea

Received 27 November 2007; revised 21 January 2008; accepted 14 February 2008

Available online 19 February 2008

Abstract—11 β -Hydroxysteroid dehydrogenase (11 β -HSD) enzymes catalyze the conversion of biologically inactive 11-ketosteroids into their active 11 β -hydroxy derivatives and vice versa. 11 β -HSD1 has been studied as a potential treatment for metabolic disease such as diabetes and obesity. To find correlation between 11 β -HSD1 and inhibitors, three-dimensional quantitative structure–activity relationship (3D-QSAR) studies were performed on 70 inhibitors, based on molecular docking conformations obtained by using FlexX-Pharm. The studies include comparative molecular field analysis (CoMFA) and comparative molecular similarity indices analysis (CoMSIA). Based on the docking results, highly predictive 3D-QSAR models were developed with q^2 values of 0.543 and 0.519 for CoMFA and CoMSIA, respectively. A comparison of the 3D-QSAR field contributions with the structural features of the binding site showed good correlation between the two analyses. Therefore, these results should be useful to the prediction of the activities of new 11 β -HSD1 inhibitors.

© 2008 Elsevier Ltd. All rights reserved.

The metabolic syndrome is increasingly recognized as a major cause of cardiovascular disease and type 2 diabetes. Recently, 11 β -Hydroxysteroid dehydrogenase type 1 (11 β -HSD1) has attracted significant attention from the pharmaceutical research as a target for the treatment of metabolic disease^{1–3} and the significance of 11 β -HSD1 in metabolic diseases such as type 2 diabetes and obesity has been demonstrated in various rodent studies.^{4–6} The enzyme 11 β -HSD1, which is mainly expressed in liver and adipose tissue, plays a central role in regulating intracellular concentrations of glucocorticoids by converting inactive cortisone to the metabolically active hormone cortisol. The type II isoform (11 β -HSD2) is located primarily in the kidney and catalyzes the inactivation of cortisol. Therefore, inhibitors of 11 β -HSD1 are being examined as the potential treatment for metabolic syndrome, diabetes, obesity, and other indications.

In this paper, we carried out molecular docking study and then 3D-QSAR models were constructed by using approaches of comparative molecular field analysis (CoMFA) and comparative molecular similarity analysis (CoMSIA) using the docking results. So it is possible

to get new insights into the relationship between the structural information of the series of 70 compounds.

A set of 70 compounds, which covered 4 log orders ($\text{pIC}_{50} = 4 \sim 8$) for their enzyme inhibitory activity, was selected from among published 11 β -HSD1 inhibitors.^{7–13} The dataset of 70 compounds was grouped into training set and test set containing 50 and 20 compounds, respectively. Both the training and the test sets were divided according to a representative range of biological activities and structural variations. These compounds' inhibitory activities were converted into the corresponding pIC_{50} ($-\log \text{IC}_{50}$) values in the CoMFA and CoMSIA analyses. These inhibitors were constructed by using molecular modeling software package Sybyl7.3.1¹⁴ and energy minimizations were carried out using Tripos force field¹⁵ and the Gasteiger–Huckel charge with a distance-dependent dielectric and conjugate gradient method.

FlexX-Pharm¹⁶ employed a fast algorithm for flexible docking of small ligands into fixed protein-binding site using an incremental construction process. This program was interfaced with Sybyl 7.3.1 and was used for docking of all of the 11 β -HSD1 inhibitors at the active site. To understand the binding mode of 11 β -HSD1 inhibitors, we analyzed all the known crystal structure including cortisol. As shown in Figure 1, two extension directions, which are hydrophobic pocket II

Keywords: 11 β -HSD1; 3D-QSAR; Docking; Inhibitor design.

*Corresponding author. Tel.: +82 42 860 7452; fax: +82 42 860 7635; e-mail: nskang@kRICT.re.kr

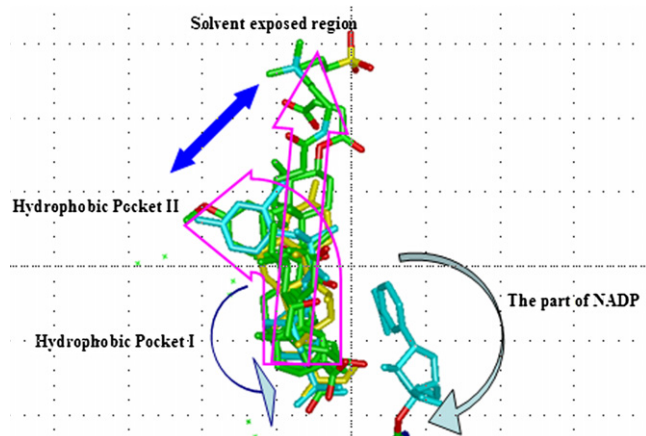


Figure 1. The superposition of the known inhibitors extracted from X-ray co-crystallized structure. The extension direction of inhibitors based on the hydrophobic pocket I is considered as two parts, one is hydrophobic pocket II, the other is the solvent exposed region.

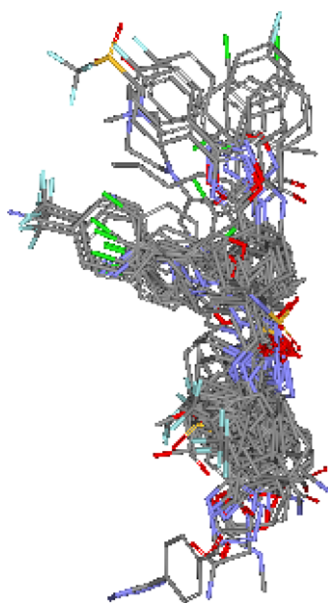


Figure 2. The 3D superimposed structures of the used compounds.

and solvent exposed region, are considered as the binding mode of its inhibitors against 11 β -HSD1. The X-ray crystal structures of 3 human 11 β -HSD1 complexes with ligands were retrieved from the PDB (PDB entry; 2BEL, 2IRW, 2ILT). The active site was defined as including all atoms within a 6.5 Å radius of the cocrystallized ligand (PDB ID:2ILT)¹⁷ and NADP was mentioned in order to obtain the appropriate bioactive conformation of the ligand within the active site. For docking with FlexX-Pharm, the most critical interactions between ligands and 11 β -HSD1 were mapped in crystal structures. The default SYBYL/FlexX parameters were used.

All the molecules in a database containing both training and test sets were docked into the active site, and 30 con-

formations were obtained through FlexX-Pharm for each ligand. The conformation was selected as the most probable binding conformation. These conformations were aligned together inside active site and used directly for CoMFA¹⁸ and CoMSIA¹⁹ analyses.

The steric and electrostatic interactions for CoMFA were calculated using the Tripos force field with a distance-dependent dielectric constant at all intersections in a different grid taking a sp^3 carbon atom as steric probe and a +1 charge as electrostatic probe. In CoMFA, when the grid spacing changed, a shift in the r^2 values is observed. So in this paper we used the different grid boxes with 1.0, 1.5, and 2.0 Å grid spacing, respec-

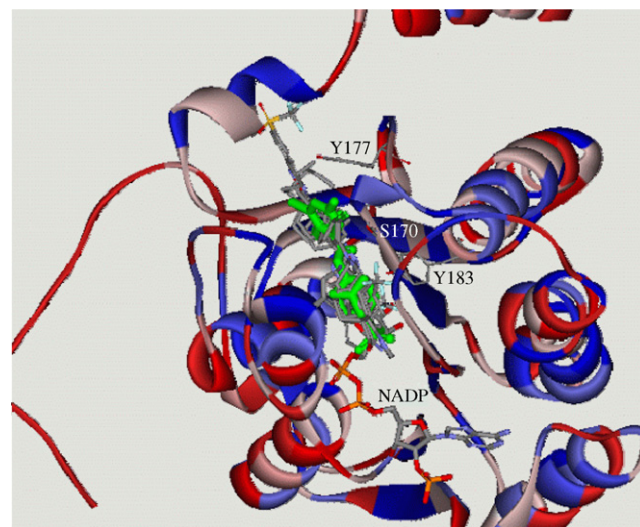


Figure 3. The docking of active compounds (7–8, 23, 42, 52, 56, 60) compared with X-ray crystallized structure. Green colored compound is the reference structure deposited in the protein data bank, 2ILT.

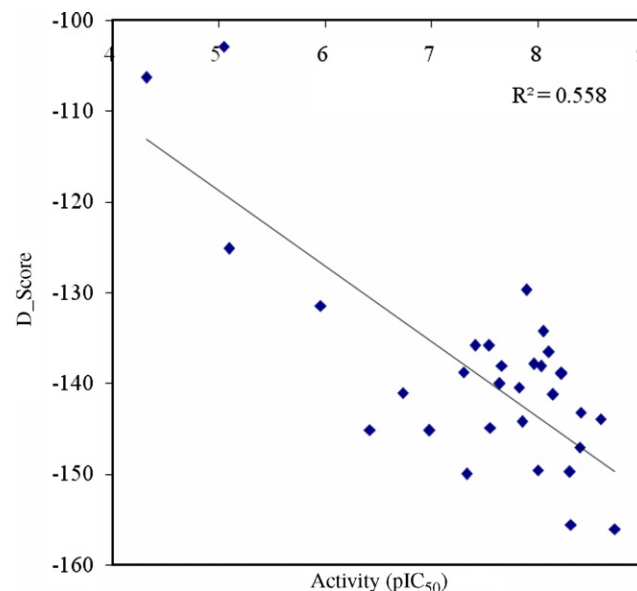
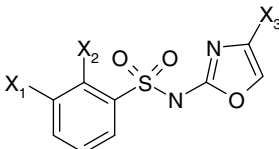
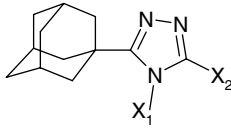
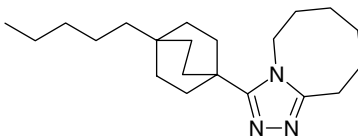
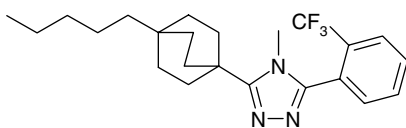
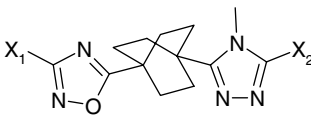
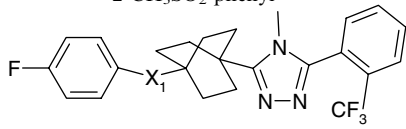
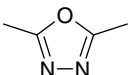
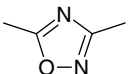
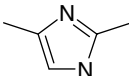
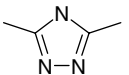


Figure 4. D_Score obtained for 32 compounds in active site of 11 β -HSD1.

Table 1. Structures of **11b**-HSD1 inhibitors used in this study

Compound	Structure			pIC ₅₀
				
	X ₁	X ₂	X ₃	
1	Cl	Methyl	4-(CN)phenyl	4.32
2^a	H	H	Phenyl	4.64
3	H	H	4-(CF ₃)phenyl	5.05
				
	X ₁	X ₂		
4	Ethyl	Propyl		7.28
5^a	Propyl	Ethyl		7.96
6^a	Butyl	Methyl		7.14
				8.30
				8.70
				
	X ₁	X ₂		
9	4-Cl-phenyl	2-CF ₃ -phenyl		8.40
10	2,4-di-F-Phenyl	2-CF ₃ -phenyl		8.59
11^a	4-F-phenyl	2-CH ₃ O-4-OH-phenyl		8.07
12	4-F-phenyl	2-CHF ₂ O-phenyl		8.03
13	4-F-phenyl	2-Cl-4-CHO-phenyl		7.66
14	4-F-phenyl	2-CH ₃ SO ₂ -phenyl		8.01
				
	X ₁			
15				8.14
16^a				8.70
17^a				8.28
18^a				8.33

(continued on next page)

Table 1 (continued)

Compound	Structure	pIC ₅₀
	X ₁	
19		7.70
20		8.39
21		8.31
22 ^a		8.38
23		8.72
	X ₁	
24		7.64
25		7.01
26		6.79
27		7.06
28		7.36
29		7.21

Table 1 (continued)

Compound	Structure	pIC ₅₀
30		7.89
31 ^a		7.66
32		8.30
33 ^a		7.60
34		7.82
35		7.96
36		6.98
37		7.41
38 ^a		7.35
39 ^a		7.39
40		7.05
41 ^a		7.46
42		8.00

(continued on next page)

Table 1 (continued)

Compound	Structure	pIC ₅₀
	X ₁	
43 ^a		8.22
44		7.55
45		7.36
46		6.73
47 ^a		8.30
48 ^a		7.85
49		7.33
50		7.54
	X ₁ X ₂	
51	COOH H	7.41
52	CONH ₂ H	8.30
53	COOH 2-Cl	8.10
54	COOH 3-Cl	7.82
55	COOH 4-Cl	7.66
56	CONH ₂ 4-Cl	8.22
57	CONH ₂ 4-OCH ₃	8.22
58 ^a		7.80
59		7.92
60	CH ₂ OH 4-Cl	8.05
61	CH ₂ OCH ₂ CO ₂ H 4-Cl	6.96
62		7.96

Table 1 (continued)

Compound	Structure	pIC ₅₀
	X ₁	
63	Methyl	5.10
64 ^a	Ethyl	5.97
	X ₁ X ₂	
65	H Cl	5.96
66 ^a	Cl H	5.80
67		7.85
68		6.42
69		7.30
70 ^a		6.74

^a Test set.

tively, were used for the CoMFA calculations. The influence of the different grid spacing on the CoMFA model is shown in Table 3. The cutoff was set to 30 kcal/mol. With standard options for scaling of variables, the regression analysis was carried out using the full cross-validated partial least-squares (PLS) method of LOO (leave-one-out). The minimum-sigma was set to 2.0 kcal/mol to improve the signal-to-noise ratio by omitting those lattice points whose energy variation was below this threshold. The final model was developed with the optimum number of components to yield a noncross-validated r^2 value. In CoMSIA, a distance-dependent Gaussian-type physicochemical property has been adopted to avoid singularities at the atomic positions and dramatic changes of potential energy for those grids in the proximity of the surface. The steric, electrostatic, hydrophobic, hydrogen-bond donor and

hydrogen-bond acceptor potential fields were calculated at each lattice intersection of a regularly spaced grid of 2.0 Å. The probe atoms with radius 1.0 Å and +1 charge with hydrophobicity of +1 and hydrogen-bond donor and hydrogen-bond acceptor properties of +1 were used to calculate five fields. Gaussian-type distance dependence and the default value of the attenuation factor ($\alpha = 0.3$) were used.

In order to determine the probable binding conformations of these inhibitors, we used FlexX-Pharm program. The docking reliability was validated using the known X-ray structure (PDB ID:2ILT) of 11 β -HSD1 in complex with a small molecular ligand NN1. The ligand was re-docked to the binding site of protein and the docked conformation corresponding to the lowest free energies was selected as the most probable binding

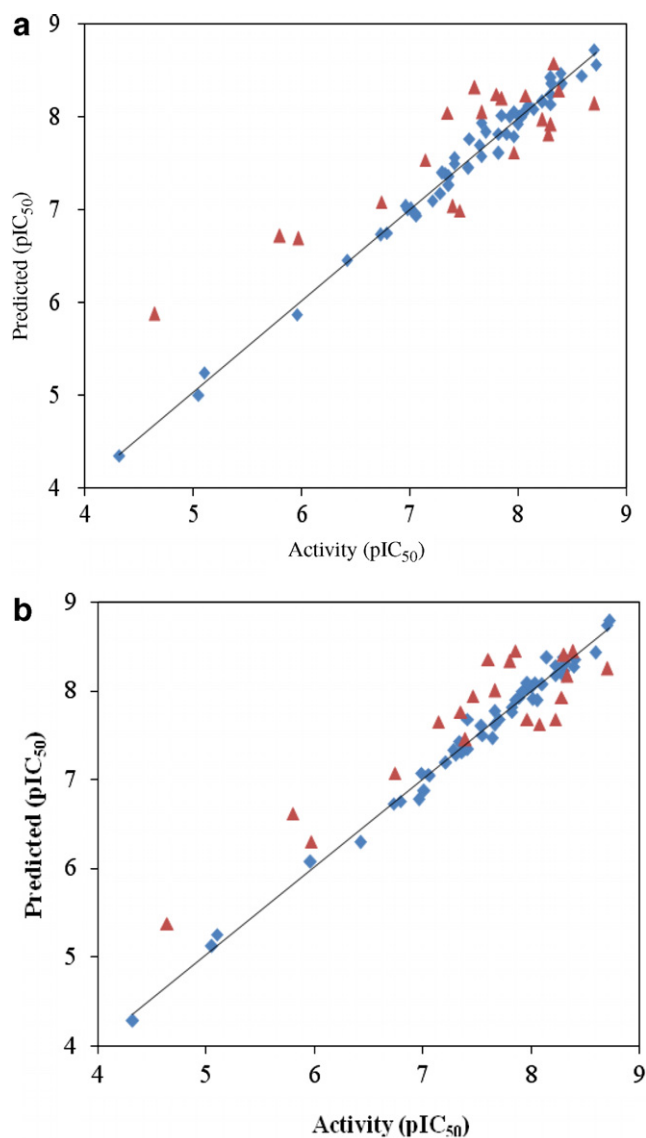


Figure 5. Correlation between actual pIC_{50} and predicted pIC_{50} from training (blue square) and test set (red triangle) (a) CoMFA; (b) CoMSIA.

Table 2. Experimental activities (pIC_{50}) and predicted activities with residual by CoMFA and CoMSIA studies

Compound	pIC_{50}	CoMFA		CoMSIA	
		Predicted	Residual	Predicted	Residual
1	4.32	4.35	−0.03	4.28	0.04
2 ^a	4.64	5.876	−1.24	5.38	−0.74
3	5.05	5.00	0.05	5.12	−0.07
4	7.28	7.18	0.10	7.33	−0.05
5 ^a	7.96	7.621	0.34	7.68	0.29
6 ^a	7.14	7.541	−0.40	7.65	−0.51
7	8.30	8.14	0.16	8.23	0.07
8	8.70	8.73	−0.03	8.74	−0.04
9	8.40	8.36	0.04	8.36	0.04
10	8.59	8.45	0.14	8.43	0.16
11 ^a	8.07	8.237	−0.17	7.62	0.45
12	8.03	8.01	0.02	8.09	−0.06
13	7.66	7.58	0.08	7.62	0.04
14	8.01	8.00	0.01	7.91	0.11
15	8.14	8.09	0.05	8.37	−0.23

Table 2 (continued)

Compound	pIC_{50}	CoMFA		CoMSIA	
		Predicted	Residual	Predicted	Residual
16 ^a	8.70	8.147	0.55	8.25	0.45
17 ^a	8.28	7.811	0.47	7.92	0.36
18 ^a	8.33	8.579	−0.25	8.17	0.17
19	7.70	7.84	−0.14	7.68	0.02
20	8.39	8.48	−0.08	8.27	0.12
21	8.31	8.36	−0.05	8.31	0.00
22 ^a	8.38	8.286	0.09	8.44	−0.06
23	8.72	8.57	0.15	8.78	−0.06
24	7.64	7.70	−0.06	7.46	0.18
25	7.01	7.01	0.00	6.87	0.14
26	6.79	6.75	0.04	6.75	0.04
27	7.06	6.94	0.12	7.05	0.01
28	7.36	7.36	0.00	7.30	0.06
29	7.21	7.10	0.11	7.19	0.02
30	7.89	7.82	0.07	7.92	−0.03
31 ^a	7.66	8.056	−0.40	8.00	−0.34
32	8.30	8.43	−0.13	8.38	−0.08
33 ^a	7.60	8.323	−0.72	8.35	−0.75
34	7.82	7.82	0.00	7.82	0.00
35	7.96	8.06	−0.10	8.02	−0.06
36	6.98	7.01	−0.03	7.07	−0.09
37	7.41	7.50	−0.09	7.34	0.07
38 ^a	7.35	8.045	−0.70	7.76	−0.41
39	7.39	7.04	0.35	7.45	−0.06
40	7.05	6.96	0.09	7.06	−0.01
41 ^a	7.46	6.995	0.47	7.94	−0.48
42	8.00	7.93	0.07	8.04	−0.04
43 ^a	8.22	7.976	0.24	7.68	0.55
44	7.55	7.76	−0.21	7.49	0.06
45	7.36	7.26	0.10	7.39	−0.03
46	6.73	6.73	0.00	6.73	0.00
47 ^a	8.30	7.923	0.38	8.40	−0.10
48 ^a	7.85	8.201	−0.35	8.45	−0.60
49	7.33	7.39	−0.06	7.43	−0.10
50	7.54	7.46	0.09	7.60	−0.06
51	7.41	7.56	−0.15	7.68	−0.27
52	8.30	8.25	0.05	8.17	0.13
53	8.10	8.12	−0.02	8.07	0.03
54	7.82	7.61	0.21	7.76	0.06
55	7.66	7.94	−0.28	7.77	−0.11
56	8.22	8.17	0.05	8.28	−0.06
57	8.22	8.18	0.04	8.17	0.05
58 ^a	7.80	8.244	−0.44	8.33	−0.53
59	7.92	8.01	−0.09	8.00	−0.08
60	8.05	8.04	0.01	7.89	0.16
61	6.96	7.04	−0.08	6.77	0.19
62	7.96	7.79	0.17	8.08	−0.12
63	5.10	5.25	−0.15	5.25	−0.15
64 ^a	5.97	6.69	−0.72	6.30	−0.33
65	5.96	5.87	0.09	6.07	−0.11
66 ^a	5.80	6.718	−0.92	6.62	−0.82
67	7.85	8.02	−0.17	7.90	−0.05
68	6.42	6.46	−0.04	6.29	0.13
69	7.30	7.40	−0.10	7.28	0.02
70 ^a	6.74	7.082	−0.34	7.07	−0.33

^a Test set.

conformation. The root-mean-square deviation (RMSD) of the docked conformation to the experimental conformation was 1.18 Å, suggesting that a high docking reliability of FlexX-Pharm in reproducing the experimentally observed binding mode for 11 β -HSD1 inhibitors and the parameter set for the FlexX-Pharm

simulation is reasonable to reproduce the X-ray structure. The FlexX-Pharm method and the parameter set could be extended to search protein-binding conformation for other inhibitors. In this study, for FlexX-Pharm constraints, four residues (SER170, TYR177, VAL180, and TYR183) were selected. The H-bond donor of SER170 was set as essential constraint, while the

phenyl_center of TYR 177 and TYR 183 and ch3_phe of VAL180 were set as optional. Thirty-two compounds in the training set considering structural varieties were chosen to decide the docking conformation using the above-mentioned docking strategy. In Figure 2, the result of docking study was shown. The r^2 value of 0.56 was obtained and thus we used the docked conforma-

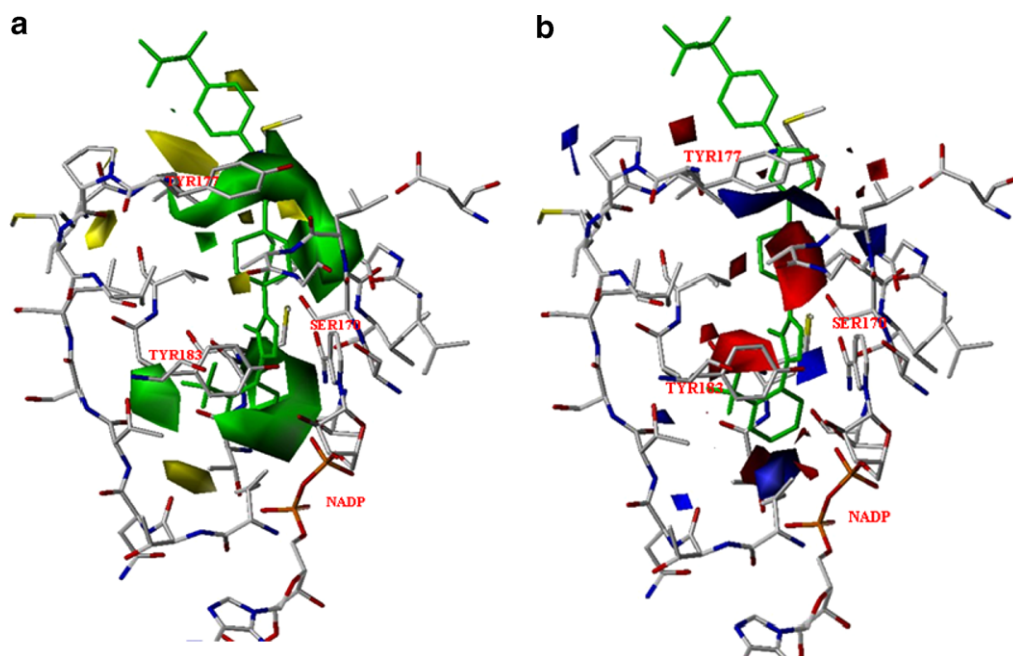


Figure 6. CoMFA contour map displayed with the compound **23** and superimposition in the active site residues of 11β-HSD1 for (a) steric contour map; (b) electrostatic contour map.

Table 3. Summary of CoMFA and CoMSIA results for various models

Component		CoMFA		CoMSIA		
				SE	SEDA	S ^e E ^h D ⁱ A ^j H ^k
Grid spacing (Å)	1	1.5	2	2	2	2
<i>q</i> ^{2a}	0.536	0.543	0.418	0.481	0.488	0.519
NOC ^b	5	5	6	6	6	6
<i>r</i> ^{2c}	0.985	0.987	0.991	0.975	0.986	0.988
SEE ^d	0.118	0.110	0.090	0.154	0.117	0.105
<i>F</i> ^e	573.372	654.615	824.504	276.991	487.312	598.511
<i>Field contribution (%)</i>						
Steric	36.5	33.9	36.8	24.8	11.7	7.9
Electrostatic	63.5	66.1	63.2	75.2	39.3	28.3
Donor	—	—	—	—	27.6	24.2
Acceptor	—	—	—	—	21.4	16.2
Hydrophobic	—	—	—	—	—	23.4
<i>r</i> _{pred} ^{2f}		0.764				0.829

^a CV correlation coefficient.

^b Number of components.

^c Correlation coefficient.

^d Standard error of estimate.

^e F -ratio.

^f Correlation coefficient of test set.

^g Steric field.

^h Electrostatic field.

ⁱ H-bond donor field.

^j H-bond acceptor field.

^k Hydrophobic field.

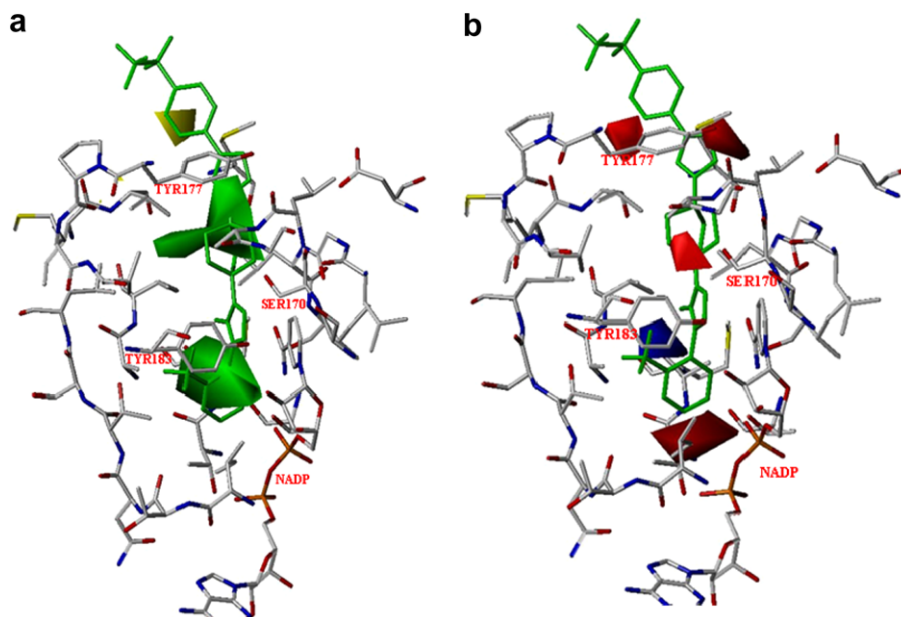


Figure 7. CoMSIA contour map displayed with the compound 23 and superimposition in the active site residues of 11 β -HSD1 for (a) steric contour map; (b) electrostatic contour map.

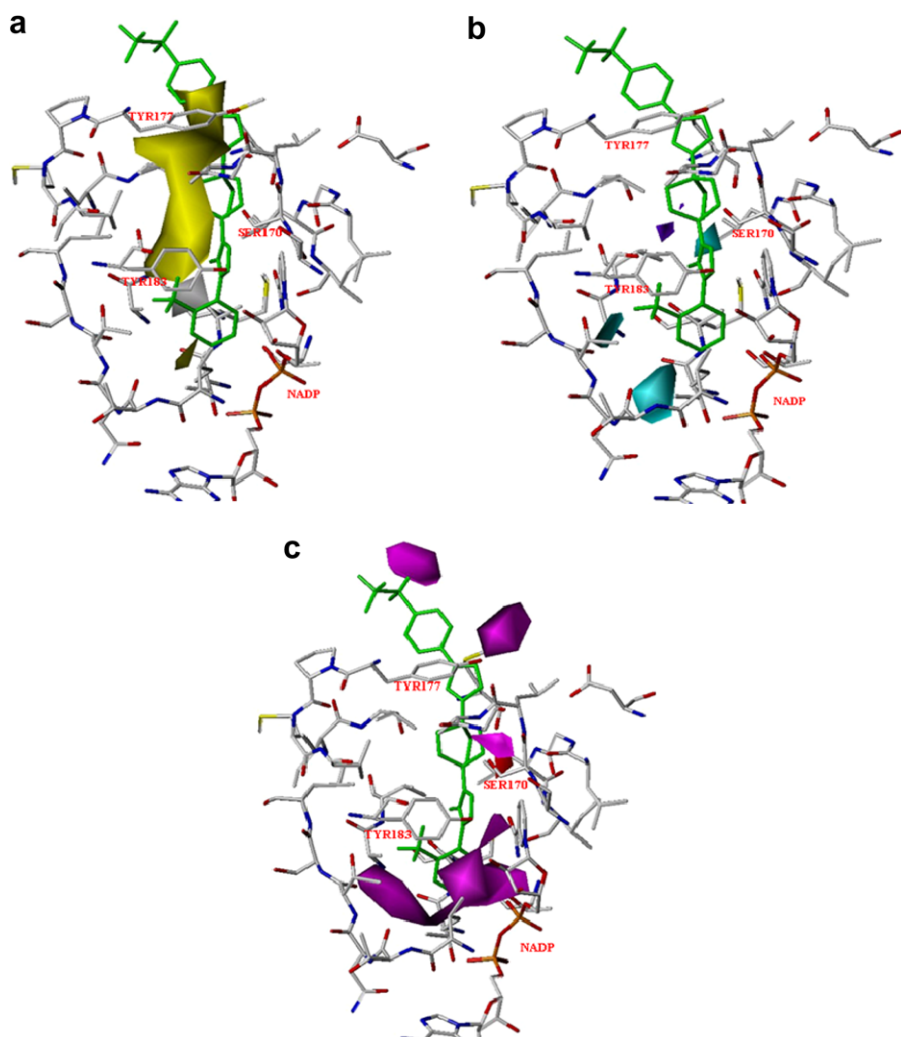


Figure 8. CoMSIA contour map displayed with the compound 23 and superimposition in the active site residues of 11 β -HSD1 for (a) hydrophobic contour map; (b) hydrogen-donor contour map; (c) hydrogen-acceptor contour map.

tions as the initial conformations for 3D-QSAR studies. The alignments of the used molecules obtained from the docking study are represented in Figures 3 and 4. Specially, in Figure 4, docking conformations of active compounds (7–8, 23, 42, 52, 56, 60) are compared with X-ray crystallized structure (green color). Totally, the alignments from docking study corresponded with the before-mentioned binding mode in Figure 1 (see Table 1).

For training set, PLS analysis results are listed in Table 3, which show a CoMFA model with a cross-validated q^2 of 0.543 with a grid spacing 1.5 Å. The noncross-validated PLS analysis with the optimum components of 5 revealed a conventional r^2 value of 0.987, $F = 654.615$, and an estimated standard error of 0.110. The steric field descriptors explain 33.9% of the variance, while the electrostatic descriptors explain 66.1%. Figure 5a shows correlation between the actual values and the predicted values and the calculated results are also listed in Table 2. The CoMFA contour plots of steric and electrostatic interactions are shown in Figure 6. To aid in visualization, the most active compound (23) is displayed with green color in the map. The green contour near

Tyr183 indicates that more bulky substituents in these positions could significantly improve the molecular biological activities. Thus, compounds 23 and 52 with bulkier substituents such as CF_3 or adamantane at this position are more active. The electrostatic contours, in which blue color represents regions where an increased positive charge is favorable for inhibitory activity and red color (represents) regions where an increased negative charge is favorable for the activity, are shown in Figure 6b. Figure 6b shows that there is a red-colored region situated close to Ser177, that is to say, the Ser177 acts as hydrogen donor so that the negative substituents should strengthen the binding of the inhibitors.

CoMSIA analysis computed the steric and electrostatic field, as in CoMFA, but it also computes additional hydrophobic, hydrogen-bond donor, and hydrogen-bond acceptor fields. The CoMSIA results are also summarized in Table 3. The CoMSIA model showed leave-one-out cross-validation q^2 and conventional r^2 values of 0.519 and 0.988 when all the five descriptors were used. The F value and standard error of estimation are 598.511 and 0.105, respectively. These data indicate

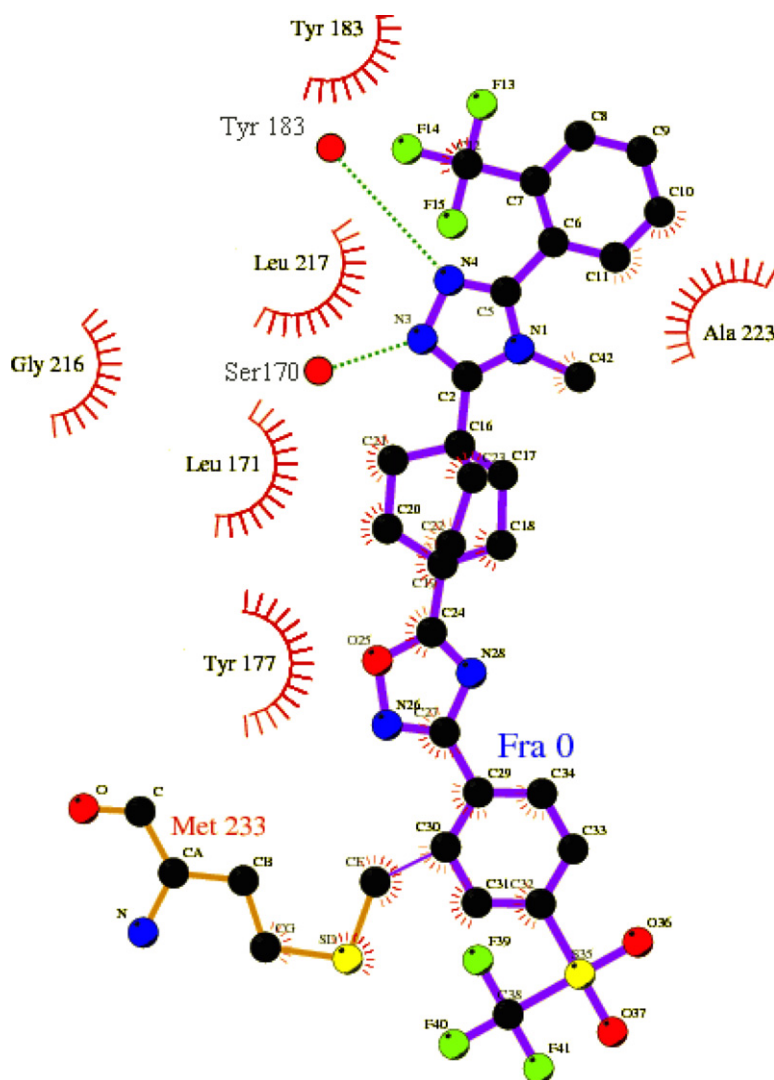


Figure 9. The subsites are labeled, the broken lines represent hydrogen-bonding interactions. The figure was drawn using the program LIGPLOT.²⁰

that a reliable CoMSIA model was successfully constructed. Figure 5b shows correlation between the actual values and the predicted values and the calculated results are also listed in Table 2. The steric and electrostatic contour maps from the CoMSIA analysis (Fig. 7) are generally in accordance with the field distributions of CoMFA maps (Fig. 6). Thus, the discussion of the CoMSIA result would be focused on hydrophobic, hydrogen-bond donor, and acceptor interactions. Figure 8a shows a superimposition of the hydrophobic CoMSIA field with the active site. Yellow contours refer to areas where the hydrophobic substituents are favorable to improve inhibitor activities, while the white contours indicate the area where hydrophilic substituents are favorable to increase inhibitory activity. The yellow contour is surrounded by the hydrophobic pocket formed by Leu126, Val180, and Tyr183. Figure 8b and c shows a superimposition of the hydrogen-bond donor and acceptor CoMSIA field with the active site. In Figure 8c, contour map for the hydrogen-bond acceptor properties highlighted in magenta represents regions where hydrogen-bond donors are expected on the receptor site. This is satisfied by the presence of Ser170 near the magenta maps. To clarify the 'favorable' binding between 11 β -HSD1 and compound 23 shown Figures 6–8, 2D schematic representation using LIGPLOT²⁰ program is given in Figure 9.

In this work, using the alignment scheme generated from the docking study, highly predictive CoMFA and CoMSIA models were developed on 11 β -HSD1 inhibitors. The satisfactory models of CoMFA and CoMSIA were obtained with leave-one-out (LOO) cross-validated q^2 values of 0.543 and 0.519, respectively, and the non-cross-validated PLS analyses with the optimum components of 5 and 6 having conventional r^2 values of 0.987 and 0.988, respectively. These models match well with the 3D topology of the binding site of 11 β -HSD1 and both models showed similar predictive capabilities. According to this study, we have established the 3D-QSAR models for 11 β -HSD1 inhibitors and the built model will be used for virtual screening to find 11 β -HSD1 inhibitors.

Acknowledgment

This research was supported by the Center for Biological Modulators of the 21st Century Frontier R&D Program, the Ministry of Science and Technology, Korea.

References and notes

- Walker, B. R.; Seckl, J. R. *Expert Opin. Ther. Targets* **2003**, 7, 771.
- Fotsch, C.; Askew, B. C.; Chen, J. J. *Exp. Opin. Ther. Patents* **2005**, 15, 289.
- Barf, T.; Williams, M. *Drugs Future* **2006**, 31, 231.
- Kotelevtsev, Y.; Holmes, M. C.; Burchell, A.; Houston, P. M.; Schmoll, D.; Jamieson, P.; Best, R.; Brown, R.; Edwards, C. R. W.; Seckl, J. R.; Mullins, J. J. *Proc. Natl. Acad. Sci. U.S.A.* **1997**, 94, 14924.
- Masuzaki, H.; Paterson, J.; Shinyama, H.; Morton, N. M.; Mullins, J. J.; Seckl, J. R.; Flier, J. S. *Science* **2001**, 294, 2166.
- Alberts, P.; Engblom, L.; Edling, N.; Forsgren, M.; Klingström, G.; Larsson, C.; Rönquist-Nii, Y.; Öhman, B.; Abrahamse'n, L. *Diabetologia* **2002**, 45, 1528.
- Xiang, J.; Ipek, M.; Suri, V.; Massefski, W.; Pan, N.; Ge, Y.; Tam, M.; Xing, Y.; Tobin, J. F.; Xu, X.; Tam, S. *Bioorg. Med. Chem. Lett.* **2005**, 15, 2865.
- Olson, S.; Aster, S. D.; Brown, K.; Carbin, I.; Graham, D. W.; Hermanowski-Vosatka, A.; LeGrand, C. B.; Mundt, S. S.; Robbins, M. A.; Schaeffer, J. M.; Slossberg, L. H.; Szymonifka, M. J.; Thieringer, R.; Wright, S. D.; Balkovec, J. M. *Bioorg. Med. Chem. Lett.* **2005**, 15, 4359.
- Gu, X.; Dragovic, J.; Koo, G. C.; Koprak, S. L.; LeGrand, C.; Mundt, S. S.; Kashmira, S.; Springer, M. S.; Tan, E. Y.; Thieringer, R.; Hermanowski-Vosatka, A.; Zokian, H. J.; Balkovec, J. M.; Waddell, S. T. *Bioorg. Med. Chem. Lett.* **2005**, 15, 5266.
- Yeh, V. S. C.; Kurukulasuriya, R.; Madar, D.; Patel, J. R.; Fung, S.; Monzon, K.; Chiou, W.; Wang, J.; Jacobson, P.; Sham, H. L.; Link, J. T. *Bioorg. Med. Chem. Lett.* **2006**, 16, 5408.
- Yeh, V. S. C.; Patel, J. R.; Yong, H.; Kurukulasuriya, R.; Fung, S.; Monzon, K.; Chiou, W.; Wang, J.; Stolarik, D.; Imade, H.; Beno, D.; Brune, M.; Jacobson, P.; Sham, H.; Link, J. T. *Bioorg. Med. Chem. Lett.* **2006**, 16, 5414.
- Patel, J. R.; Shuai, Q.; Dinges, J.; Winn, M.; Plushchev, M.; Fung, S.; Monzon, K.; Chiou, W.; Wang, J.; Pan, L.; Wagaw, S.; Engstrom, K.; Kerdesky, F. A.; Longenecker, K.; Judge, R.; Qin, W.; Imade, H. M.; Stolarik, D.; Beno, D. W. A.; Brune, M.; Chovan, L. E.; Sham, H. L.; Jacobson, P.; Link, J. T. *Bioorg. Med. Chem. Lett.* **2007**, 17, 750.
- Coppola, G. M.; Kukkola, P. J.; Stanton, J. L.; Neubert, A. D.; Marcopulos, N.; Bilci, N. A.; Wang, H.; Tomaselli, H. C.; Tan, J.; Aicher, T. D.; Knorr, D. C.; Jeng, A. Y.; Dardik, B.; Chatelain, R. E. *J. Med. Chem.* **2005**, 48, 6696.
- SYBYL 7.3.1 Tripos Inc., St. Louis, MO 63144, USA.
- Clark, M.; Cramer, R. D.; Leach, A. R.; Opdenbosch, N. V. *J. Comput. Chem.* **1989**, 10, 982.
- Hindle, S.; Rarey, M.; Buning, C.; Lengauer, T. *J. Comput. Aided Mol. Des.* **2002**, 16, 129.
- Sorensen, B.; Winn, M.; Rohde, J.; Shuai, Q.; Wang, J.; Fung, S.; Monzon, K.; Chiou, W.; Stolarik, D.; Imade, H.; Pan, L.; Deng, X.; Chovan, L.; Longenecker, K.; Judeg, R.; Qin, W.; Brune, M.; Camp, H.; Frevert, E. U.; Jacobson, P.; Link, J. T. *Bioorg. Med. Chem. Lett.* **2007**, 17, 527.
- Cramer, R. D.; Patterson, D. E.; Bunce, J. D. *J. Med. Chem. Soc.* **1988**, 110, 5959.
- Klebe, G.; Abraham, U. *J. Comput. Aided Mol. Des.* **1999**, 13, 1.
- Wallace, A. C.; Laskowski, R. A.; Thornton, J. M. *Protein Eng.* **1995**, 8, 127 (Ligplot).